JRRD
Volume 50, Number 5, 2013
Pages 651–662

Coordination patterns of shoulder muscles during level-ground and incline wheelchair propulsion

Liping Qi, PhD;[1–2] James Wakeling, PhD;[3] Simon Grange, PhD;[1–2] Martin Ferguson-Pell, PhD[2*]
[1]ASPIRE Centre for Disability Sciences, Institute of Orthopedics and Musculoskeletal Science, University College London, Brockley Hill, Stanmore, London, United Kingdom; [2]Faculty of Rehabilitation Medicine, University of Alberta, Edmonton, Alberta, Canada; [3]Department of Biomedical Physiology and Kinesiology, Simon Fraser University, Burnaby, British Columbia, Canada

Abstract—The aim of this study was to investigate how the coordination patterns of shoulder muscles change with level-ground and incline wheelchair propulsion. Wheelchair kinetics and electromyography (EMG) activity of seven muscles were recorded with surface electrodes for 15 nondisabled subjects during wheelchair propulsion on a stationary ergometer and wooden ramp (4 degree slope). Kinetic data were measured by a SmartWheel. The kinetics variables and the onset, cessation, and duration of EMG activity from seven muscles were compared with paired *t*-tests for two sessions. Muscle coordination patterns across seven muscles were analyzed by principal component analysis. Push forces on the push rim and the percentage of push phase in the cycle increased significantly during incline propulsion. Propulsion condition and posture affected muscle coordination patterns. During incline propulsion, there was more intense and longer EMG activity of push muscles in the push phase and less EMG activity of the recovery muscles, which corresponded with the increased kinetic data total force output and longer push phase in the incline condition. This work establishes a framework for developing a performance feedback system for wheelchair users to better coordinate their muscle patterning activity.

Key words: electromyography, ergometer, kinetics, muscle synergy, principal component analysis, propulsion, rehabilitation, shoulder, wavelet analysis, wheelchair.

INTRODUCTION

People with spinal cord injury (SCI) usually rely on their ability to propel a manual wheelchair for independent mobility [1]. Achieving the highest degree of independence in a manual wheelchair often depends on the user's ability to negotiate a range of environments and overcome indoor and outdoor obstacles. Ramps of varying degrees are frequent both outdoors and indoors. Laboratory investigations have revealed that shoulder joint forces [2–4] and muscle demands [5] are greater during incline propulsion than during level-ground propulsion. Wheelchair users also adopt different postures and employ different stroke techniques to suit different locomotion tasks [6]. When moving up a ramp, they tend to lean forward more than when rolling along a level surface,

Abbreviations: AD = anterior deltoid, BB = biceps brachii, EMG = electromyography, MD = middle deltoid, ME = mechanical effectiveness, MVC = maximum voluntary isometric contraction, PC = principal component, PCA = principal component analysis, PD = posterior deltoid, PM = pectoralis major, SCI = spinal cord injury, sEMG = surface electromyography, TB = triceps brachii, UT = upper trapezius.

[*]**Address all correspondence to Martin Ferguson-Pell, PhD; 3-48 Corbett Hall, University of Alberta, Edmonton, Alberta, Canada T6G 2G4; 780-248-1367; fax: 780-492-1626. Email: martin.ferguson-pell@ualberta.ca**

http://dx.doi.org/10.1682/JRRD.2012.06.0109

shifting their center of gravity forward; on an incline, they tend to push the wheel by arcing strokes rather than by the semicircular motion used in level-ground propulsion. It is still unclear how shoulder muscles are coordinated to adequately perform inclined propulsion. It stands to reason, however, that the various muscles that maintain the stability of the shoulder joints through coordinated and balanced activation will all show markedly different recruitment patterns between incline and level-ground propulsion.

Surface electromyography (sEMG) is a widely used, noninvasive method for quantifying patterns of neuromuscular activation. This procedure has been applied in several studies to track shoulder muscle activity during wheelchair propulsion [7–8]. Advanced signal processing techniques have enabled the analysis of muscle coordination patterns. Wavelet analysis offers possibilities to optimize the analysis with respect to time- and frequency-resolution of the nonstationary signals [9]. When studying the patterns of activity derived from several muscles around joints, it becomes critical to develop analytical methods that compare and describe the electromyography (EMG) activity across muscles synthetically. Conventional analyses of EMG signals, particularly in the clinical setting, are rather descriptive and generally focus on determining the timing of onsets and peaks, as well as the duration of EMG bursts, and on characterizing the intensity of muscle activation by defining indexes such as the EMG peak amplitude or the integral of the EMG burst [10]. In the present study, principal component (PC) analysis (PCA) was chosen as the most suitable method for quantifying the coordination patterns across several muscles. PCA takes as input the set of muscle coordination patterns across all tested propulsion cycles and finds the PCs that describe the major features within these coordination patterns. The purpose of the present study was to investigate, using wavelet analysis and PCA, the shoulder muscle coordination patterns during level-ground versus incline wheelchair propulsion in nondisabled participants. A better understanding of muscle coordination patterns is important for developing appropriate and effective therapeutic exercise programs for wheelchair users in order to enhance their performance and to prevent injuries. To that end, shoulder muscle assessment instruments should be developed that will enable clinicians and wheelchair users to assess the users' capacity to function and provide critical feedback. The intention is that, by optimizing performance, users will both reduce the effort and expenditure of energy in routine activity with the specific aim of reducing fatigue.

METHODS

Participants

Fifteen nondisabled participants (8 males and 7 females, age: 30 ± 4 yr, weight: 65 ± 12 kg) volunteered to participate in this study. None reported any previous history of upper-limb pain or neuromuscular disorder.

Surface Electromyography

sEMG activity of upper-limb muscles was recorded using parallel-bar EMG sensors (DE-3.1 double differential sensor, 1 mm in diameter and separated by 10 mm, Bagnoli Desktop EMG System, Delsys Inc; Boston, Massachusetts). Double differential electrodes were used to reduce crosstalk from deeper muscles. sEMG signals were detected on seven muscles of the right shoulder after depilation and cleaning with alcohol wipes: anterior deltoid (AD), middle deltoid (MD), posterior deltoid (PD), pectoralis major (PM), upper trapezius (UT), biceps brachii (BB), and triceps brachii (TB). The EMG signals were recorded with a 16-bit analog-to-digital converter (NI PCI-6220, National Instruments Corporation; Austin, Texas) during wheelchair propulsion, sampled at 2 kHz.

Kinetics

To better understand the applicability of shoulder EMG data, kinetic data were integrated to confirm when certain muscles are active during different phases of wheelchair propulsion. An instrumented wheel (SmartWheel, Out-Front; Mesa, Arizona) was used to collect kinetic data. The SmartWheel is a modified mag-wheel capable of measuring three-dimensional forces and moments occurring at the push rim. The push rim kinetic data were collected at 240 Hz. Kinetic and EMG recordings were synchronized.

Procedure

Maximum Voluntary Isometric Contraction Test

To facilitate comparison between studies, maximum voluntary isometric contractions (MVCs) were performed to normalize the EMG signals [11–12]. A force transducer (model LCCB-1K, OMEGA Engineering Inc; Stamford,

Connecticut) was used to measure the force generated from isometric contractions. During these isometric contractions, participants were provided with visual feedback of their performance on a computer monitor displaying their force traces and raw EMG. The force signals were sampled at 2 kHz.

Wheelchair Propulsion at Ergometer and Ramp

Wheelchair ergometer. A test wheelchair (Quickie GP, Sunrise Medical; Fresno, California), with 56 cm (24 in.) diameter rear wheels, 13 cm (5 in.) diameter polyurethane castor wheels, 41 cm (16 in.) seat width, 41 cm (16 in.) seat depth, and 0° camber angle, was aligned and secured over the rollers of an ergometer [13]. The SmartWheel was placed on the right side of the test wheelchair. This test wheelchair was mounted on an ergometer connected to an LCD monitor placed in front of the participant to provide visual speed feedback. Participants were given ample time to get used to propelling the wheelchair and to establish a comfortable propulsion technique. Data were recorded at a speed of 1 m/s for 1 min during propulsion. This speed (1 m/s) was selected because it is close to the safe speed required to cross an intersection with traffic lights [14].

Ramp. A 4° wooden ramp, 4.1 m long and 1.3 m wide, was constructed. The ramp led to a 1.3 × 1.2 m platform. Each participant performed two trials of incline propulsion along the ramp at a self-selected speed.

Data Analysis

Kinetics Data Analysis

For this study, the propulsion cycle was divided into push phase and recovery phase [13]. For each participant, the average of 10 continuous cycles on the ergometer was used for data analysis; from incline propulsion, the average of 5 cycles was used for data analysis. The kinetic variables analyzed were mean total force (F_{tot}), mean tangential force (F_t), and mean propulsion moment (M_z) [13]. Mechanical effectiveness (ME) was calculated by F_t/F_{tot}. Percent push phase is the percentage share of the push phase in the total propulsion cycle. In addition, by using the output of the SmartWheel software, the push frequency (number of pushes per second), push length (length of hand-on to hand-off in degrees), and push time (time of each individual push in seconds) were determined.

Wavelet and Principal Component Analysis of Electromyography Signal

All signal processing was performed using custom programs written in Mathematica version 6.0 (Wolfram; Champaign, Illinois). EMG data were normalized to percentage of cycle time and synchronized with kinetic data. The EMG signals were resolved into intensities in time-frequency space using a wavelet technique [9]. A wavelet, or "little wave," is well defined in both time and frequency and has a time-integral of zero. A set of wavelets was built that had center frequencies, as calculated by:

$$f_c(k) = \frac{(k + c_1)^{c2}}{c_3} \quad ,$$

where $c1$, $c2$, and $c3$ = scaling factors and k = wavelet number. The scaling factors ($c1$, $c2$, and $c3$) took values of 1.45, 1.959, and 0.3, respectively. These center frequencies occur where the wavelets have maximum amplitude in the frequency domain. The method has been described in detail in previous articles [15–16]. The intensities of the EMG calculated from the wavelets (10–350 Hz, k = 1–10) were summed to give the total EMG intensity, and this is simply referred to as the EMG intensity. The EMG intensity is a measure of the time-varying power within the signal and is equivalent to twice the square of the root-mean-square. The EMG intensity for each participant from the MVC was calculated and used to normalize the EMG intensities for the respective participants. To determine the onset and cessation of EMG activity, a threshold (10% MVC) was computed for each muscle and each participant [16–17].

The EMG intensities were synchronized with the kinetic data and then interpolated to 100 evenly spaced points for each propulsion cycle (1%–100% cycle). The EMG intensities from all seven muscles were used to construct grids that define the muscle coordination pattern for each propulsion cycle, and PCA was used to identify predominant coordination patterns during the propulsion cycle. Normalized EMG intensities from the level-ground and incline propulsion cycles were placed into a $p \times N$ matrix **A**, where p = 700 samples per pattern (7 muscles × 100 EMG intensities per cycle) and N = number of propulsion cycles analyzed (all participants and all trials). The weightings of each PC were given by the eigenvectors (ξ) of covariance matrix **B,** and the amount of the signal explained by each PC was determined from the eigenvalues. The relative proportion of

the recruitment patterns explained by each PC was given by $\xi' B \xi$, and the loading scores for each PC for the *N* propulsion cycles were given by $\xi' A$.

The goal of this study was to identify the effect of the propulsion environment on shoulder muscle coordination. Incline versus level-ground propulsion was to be related to specific muscle coordination patterns. We postulated that when viewed within the PCA paradigm, level-ground and incline propulsion techniques require distinct patterns of muscle recruitment. Thus, the problem was reduced to identifying sets of patterns that both characterize each coordination pattern and discriminate between coordinate patterns. The EMG activation pattern of the seven tested muscles was identified from each propulsion cycle. We applied PCA to the set of 929 propulsion cycles (223 cycles from incline propulsion and 706 cycles from level-ground propulsion) and interpreted a few of the most significant components. Instead of averaging or selecting typical cycles from each muscle, PCA quantitatively classifies the coordination patterns recorded across muscles by giving PC weightings and loading scores. The PCs were calculated from the covariance matrix of the data set matrix without prior subtraction of the mean data, so the PCs describe the components of the entire signal. The smaller set of patterns are represented by PC weightings (eigenvectors), whereas the loading scores (eigenvalues) define how much of each pattern is present in the individual propulsion cycles. PC1 weightings represent the most common patterns across cycles, participants, and conditions (**Figure 1**). The variations between conditions, participants, and cycles are explained by the other PCs (**Figure 1**). Coordination patterns can be reconstructed from the vector product of the PC weightings and the PC loading scores. The coordination patterns across seven muscles for each propulsion cycle can be explained by the vector product of all the weightings and loading scores for that cycle. The EMG intensities during level-ground versus incline propulsion were reconstructed from the sum of the products of the PC weightings and their loading scores for each propulsion cycle. The mean coordination for each condition (incline vs level-ground) was reconstructed using the first 10 PCs that describe the major features of the coordinated pattern (>50% of signals). When the patterns are reconstructed for level-ground and incline propulsion, the contribution of PC weightings and loading scores are positive or negative. Positive loading scores indicate relatively more muscle activity within the common activity; negative loading scores indicate less muscle activity. PCA was used to decompose EMG activation patterns in a small set of basis patterns that capture the most relevant features of the original EMG activation patterns across muscles. In this study, the first ten PCs explain more than 50 percent of the signal.

Statistical Analysis

Statistical analysis was performed using SPSS version 16 (IBM Corporation; Armonk, New York). Kolmogorov-Smirnov and Shapiro-Wilk tests were performed to confirm data normality. Paired *t*-tests were conducted to test the significant differences of the kinetic variables and EMG onset, cessation, and duration between level-ground and incline propulsion. General linear model analyses of variance were used to test for significant differences in PC1 to PC10 loading scores between level-ground and incline propulsion with participants and cycles as random factors. In each statistical analysis, results were considered to be significant when $p < 0.05$.

RESULTS

Kinetics

Table 1 shows the mean total force (F_{tot}), mean tangential force (F_t), mean propulsion moment (M_z), push length, push time, push frequency, and ME for level-ground and incline propulsion. Total force, tangential force, propulsion moment, and push length increased significantly during incline propulsion (**Table 1**). Incline propulsion shows a significantly longer percent push cycle than level-ground propulsion. No significant differences were found in the ME between level-ground and incline propulsion.

Electromyography Activity

Incline propulsion displayed a significantly higher EMG intensity for PM, AD, BB, TB, and PD than level-ground propulsion, while MD had significantly lower EMG intensity in incline propulsion than in level-ground propulsion. No significant differences were found in EMG intensity for UT between level-ground and incline propulsion. **Table 2** shows the timing of EMG activity of seven muscles during wheelchair propulsion. Compared with level-ground propulsion, AD, PM, and BB had a significantly longer EMG duration in incline propulsion. Incline propulsion showed a significantly shorter EMG duration in UT, MD, and PD than the level-ground

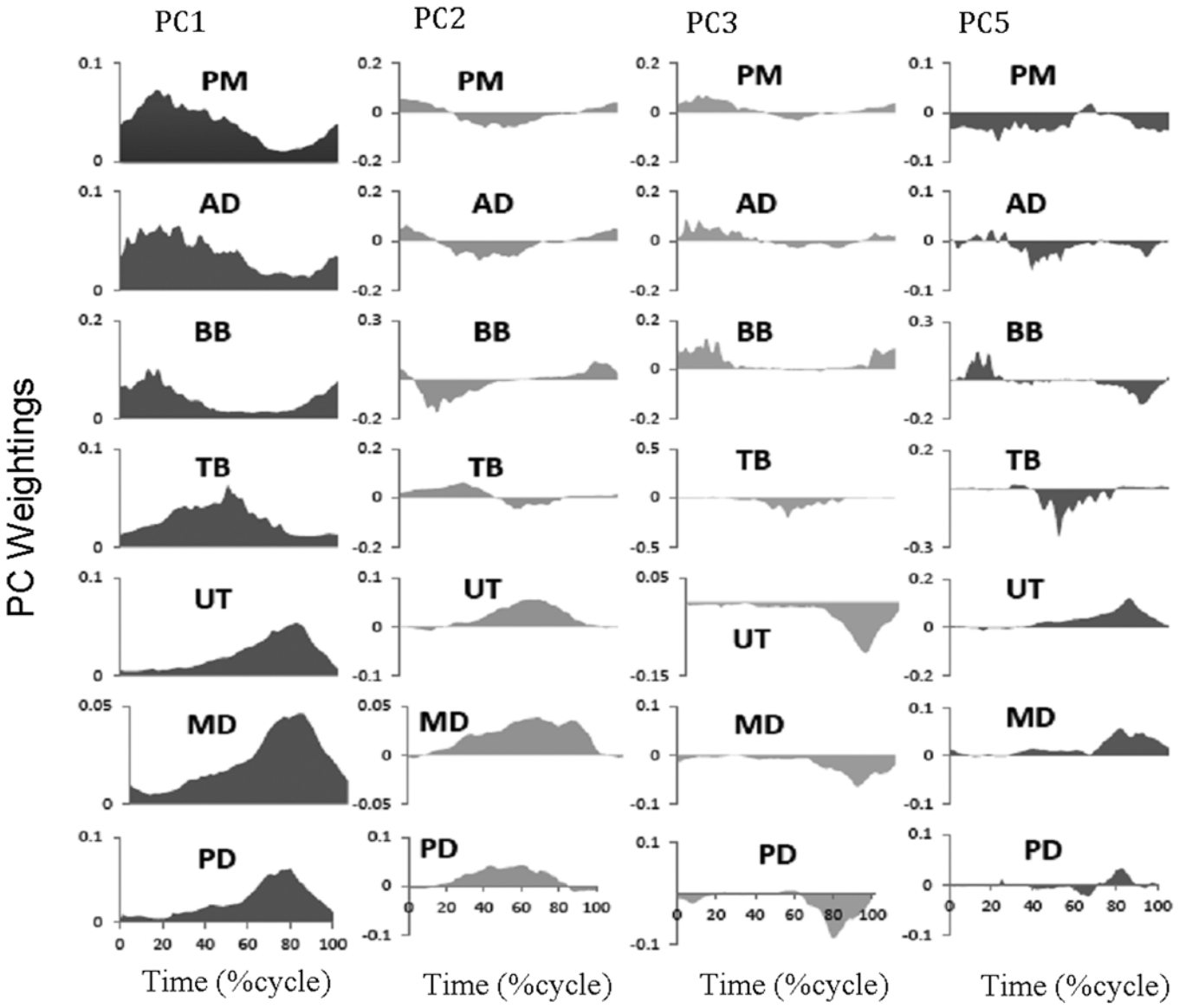

Figure 1.
Weightings of PC1, PC2, PC3, and PC5. PC1 explains 24.5 percent of overall coordination patterns. PC2, PC3, and PC5 explain 7.4, 5.3, and 3.4 percent of the overall coordination patterns, respectively. Time base of propulsion cycle was normalized to 100 percent. AD = anterior deltoid, BB = biceps brachii, MD = middle deltoid, PC = principal component, PD = posterior deltoid, PM = pectoralis major, TB = triceps brachii, UT = upper trapezius.

propulsion condition, which is consistent with the shorter percent recovery phase in incline propulsion.

PC1, PC2, PC3, PC5, PC8, and PC9 loading scores were significantly different between incline and level-ground propulsion. There was a significant interaction between the effect of propulsion conditions and random factor of subjects on PC loading scores. **Figure 1** shows the weightings of PC1, PC2, PC3, and PC5. PC1 gives a general coordination pattern, explaining 24.5 percent of the overall coordination patterns. PC2, PC3, and PC5 contain both positive and negative weightings and loading scores (**Table 3**), illustrating different types of variation in the muscle coordination patterns. PC2 explains 7.4 percent of the signal. Reconstructed with positive PC2 loading scores in level-ground propulsion, PC2 shows a relative increase in push phase muscle intensities (AD,

Table 1.
Kinetics variables for level-ground and incline propulsion. Data reported as mean ± standard deviation.

Condition	Level-Ground	Incline
Speed (m/s)	1.0 ± 0.1	0.6 ± 0.1
Total Force (N)*	33.8 ± 9.9	83.4 ± 17.5
Propulsion Moment (Nm)*	6.2 ± 1.1	17.5 ± 2.8
Tangential Force (N)*	24.1 ± 4.4	67.9 ± 12.2
Push Phase (%)*	42.9 ± 6.4	67.2 ± 6.9
Push Length (°)*	60.1 ± 7.3	67.5 ± 12.2
Push Frequency (1/s)	0.9 ± 0.1	1.0 ± 0.2
Mechanical Effectiveness	0.7 ± 0.1	0.8 ± 0.1
Push Time (s)	1.1 ± 0.2	1.1 ± 0.2

*Significant difference ($p < 0.05$).

PM, and BB) during the late recovery phase and early push phase and relatively lower EMG intensities of these muscles during the remaining part of the stroke. For the recovery phase muscles (UT, MD, and PD), PC2 weightings display relatively higher intensities coupled with a shift to the late push phase and relatively less activity during the late recovery phase. The PC2 loading score is negative in incline propulsion, and then the reverse of these effects occurs. PC3 explains 5.3 percent of the signal. PC3 weightings of the recovery muscles correspond with delayed peaks of the PC2 weightings. Reconstructed with negative PC3 loading scores in level-ground propulsion, the negative weightings of the recovery muscles display relatively higher activity during the mid to late recovery phase. Conversely, the negative PC3 weightings coupled with positive PC3 loading scores show more focused recovery muscle activity during incline propulsion. PC5 explains 3.4 percent of the signal and shows a relative decrease in AD, PM, and BB activity from late push phase to recovery phase coupled with more focused bursts of activity in UT, MD, and PD during the late recovery phase for level-ground propulsion. For propulsion up the ramp, the mean PC5 loading score is negative and so the reverse of these effects occurs: AD, PM, and TB were less active, whereas UT, MD, and PD demonstrated a burst of activity.

The EMG intensities were reconstructed from the sum of the products of the PC weightings and their loading scores for each cycle (**Table 3**), using the first 10 PCs (>50% of signals) that describe the major features of the coordination (**Figure 2**).

DISCUSSION

Motor Control Strategies Between Muscles in Different Propulsion Conditions

The shoulder muscles are activated for distinct periods within each propulsion cycle. The push phase synergy is dominated by the AD, PM, and BB [7–8], whereas UT, MD, and PD have their primary activity during the recovery phase. The significantly longer EMG duration of the push muscles during incline propulsion coincides with the longer percent push phase, which demonstrates an effective adaptive response of the synergistic muscles to the environmental requirements. In addition, EMG intensity of the push muscles increased significantly during incline propulsion, which corresponds with the increased total force output in the incline propulsion condition. It was obvious to the observer that the participants adopted the forward-leaning posture to help prevent backward tipping during incline propulsion. They used a shorter recovery phase and hastened to move their hands back to the rim to avoid rolling backward

Table 2.
Timing (percent of cycle) of electromyography activity for level-ground and incline wheelchair propulsion. Data reported as mean ± standard deviation.

Muscle	Onset		Cessation		Duration		Peak	
	Level-Ground	Incline	Level-Ground	Incline	Level-Ground	Incline	Level-Ground	Incline
Anterior Deltoid	89 ± 8	90 ± 13	28 ± 6	56 ± 13*	40 ± 9*	69 ± 10*	10 ± 8*	33 ± 20*
Pectoralis Major	86 ± 8	91 ± 10	31 ± 10	58 ± 15*	45 ± 8	67 ± 10*	19 ± 22	27 ± 11
Biceps Brachii	84 ± 14	88 ± 12	18 ± 7	35 ± 15*	33 ± 13	47 ± 12*	93 ± 10	6 ± 11*
Triceps Brachii	97 ± 3	22 ± 19*	43 ± 10	67 ± 10*	45 ± 8	45 ± 15	22 ± 13	50 ± 11*
Upper Trapezius	35 ± 9*	50 ± 15*	92 ± 4*	92 ± 6	55 ± 10	41 ± 10*	68 ± 10	71 ± 11
Middle Deltoid	26 ± 5*	41 ± 14*	92 ± 4	96 ± 8	66 ± 8	54 ± 10*	71 ± 11*	71 ± 8
Posterior Deltoid	30 ± 7*	46 ± 15*	93 ± 4	96 ± 8	62 ± 8	50 ± 11*	72 ± 12*	69 ± 9

*Significant difference ($p < 0.05$).

Table 3.
First 10 principal component (PC) loading scores of level-ground and incline propulsion and percent weightings. Data reported as mean ± standard deviation.

PC	Level-Ground	Incline	Signal Explained by PC (%)
1	21.7 ± 0.3*	56.2 ± 2.3*	24.5
2	10.5 ± 0.3*	–4.9 ± 2.4*	7.4
3	–5.7 ± 0.3*	2.3 ± 2.1*	5.3
4	–2.4 ± 0.3	–1.6 ± 1.9	4.5
5	5.3 ± 0.3*	–6.1 ± 1.6*	3.4
6	0.3 ± 0.2	0.2 ± 1.7	2.8
7	–0.2 ± 0.2	0.05 ± 1.6	2.5
8	–1.0 ± 0.3*	1.1 ± 1.2*	2.2
9	2.8 ± 0.3*	–2.4 ± 1.1*	2.2
10	0.01 ± 0.2	0.3 ± 1.2	1.8

*Significant difference ($p < 0.05$).

between pushes; this action explains the longer push phase and shorter recovery phase in incline propulsion. MD showed significantly lower EMG intensity in incline propulsion. Increased EMG intensity of PD for incline propulsion is related to the forward-leaning trunk position and downward push.

Previous investigators using measures of EMG amplitude have suggested differences in muscle recruitment between level-ground and incline propulsion, which does not directly quantify coordination across muscles [18]. In order to gain additional insight into the differences in muscle coordination between propulsion conditions, PCA was used to decompose EMG activation patterns in a small set of patterns that capture the most relevant features of the original EMG activation patterns across muscles. PCA analysis is useful to quantitatively classify EMG patterns recorded across muscles and from the same muscle across different motor tasks. The reduced number of patterns defines a low-dimensional space in which it is possible to examine the distribution of the original EMG activation patterns. PC1 weightings represent the most common pattern across cycles, participants, and conditions. The variations between conditions, participants, and cycles are explained by the other PCs. Positive or negative vector products of PC2 and PC5 in **Figure 2** and **Table 3** denote positive or negative contributions of those PCs to the coordination pattern for a specific condition. PC2 loading scores were different between the two conditions, which represents differently coordinated motor behavior between level-ground and incline propulsion. Most participants applied the semicircular stroke during level-ground propulsion, which is with their arms moving behind the body to start a push. This motion requires PM, AD, and BB muscle activity in the late recovery phase as the arms return and prepare for the next push. Visualized with PC2 weightings, mean positive PC2 loading scores in level-ground propulsion are associated with PM, AD, and BB EMG activity in the early push phase (0%–20% cycle) and late recovery phase (80%–100% cycle) and EMG activities of recovery muscles (UT, MD, and PD) in the late push phase and recovery phase (30%–80% cycle). During incline propulsion, participants adopted the arcing stroke and forward-leaning posture. With the arcing pattern, the hands remain close to the push rim when coasting, which is associated with a shorter percent recovery phase. Mean negative PC2 loading scores during incline propulsion are associated with more intense and longer EMG activity of push muscles in the push phase (30%–70% cycle) and less EMG activity of recovery muscles. Similarly, mean positive PC5 loading scores for level-ground propulsion explain relatively more AD and BB EMG activity in the early push phase (0%–20% cycle) and less EMG activity of push muscles in the recovery phase, whereas the mean negative PC5 loading scores for incline propulsion show longer EMG activity of push muscles to accommodate the significantly longer percent push phase and less EMG activity of recovery muscles in the late recovery phase (70%–100% cycle). Push and recovery muscle synergies worked differently on the ramp than in the level-ground propulsion condition, which indicates that coordinated motor behavior is regulated to match the requirements of the given movement and to allow for highly specialized and flexible motion.

In this study, we show that changes in muscle coordination are associated with propulsion conditions, with the first 10 PCs accounting for 50 percent of the EMG signal. This implies that the other 50 percent of the total EMG signal might be varied with the mechanics of the propulsion tasks, intersubject and intercycle variability, and noise from the measurement systems and data collection. Muscle activity and coordination can vary between subjects throughout a single propulsion cycle and between different cycles of the same person. With different propulsion techniques, there are variations in the muscle coordination used to complete a propulsion cycle. PCA captures most of the relevant features of the original EMG activation patterns across muscles. It is encouraging to see that PCA resolved functional differences in the coordination

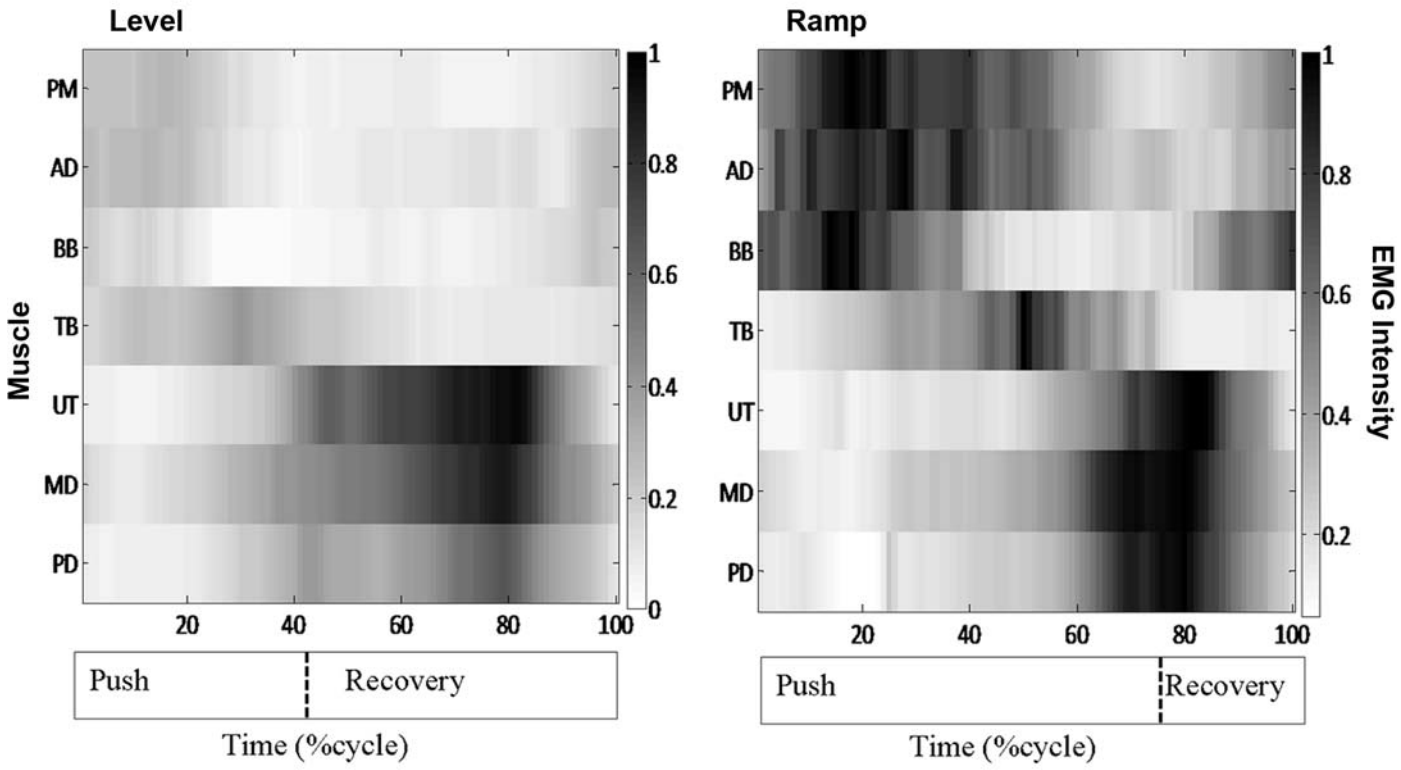

Figure 2.
Reconstructed electromyography (EMG) intensity for level-ground and incline propulsion from seven tested shoulder muscles. EMG intensity scales have been normalized to maximum intensity for each muscle in range of [0, 1], where color map represents intensity of EMG signal. Time base of propulsion cycle has been normalized to 100 percent, push phase being time elapsed between hand-on to hand-off push rim. AD = anterior deltoid, BB = biceps brachii, MD = middle deltoid, PD = posterior deltoid, PM = pectoralis major, TB = triceps brachii, UT = upper trapezius.

patterns that were not detectable using the traditional EMG statistics. This approach allows for patterns and trends in EMG characteristics to effectively and consistently map out patterns of physical activity, generating a "signature" for the activity, which can be likened to a "tomogram" of electrical activity. This approach can be extended to create a library of predicted behavior that, with machine learning, may be used to illustrate variance from predicted response to demand, and as with earlier work on the effect of fatigue [13], may be used to provide feedback to users or other control systems to better coordinate muscle patterning activity.

Limitations

The present study investigated incline propulsion with a 4° ramp. Everyday propulsion environments can involve climbing much steeper slopes. A standard access ramp into a building is 4.8° (1:12) in the United States [19]. Previous studies demonstrated that the muscular challenge for the upper limb increases with increasing ramp grades [18]. Pushing up a 2.9° ramp has been reported to require as much as 66 percent of the wheelchair user's shoulder-flexion strength [5]. Coordination patterns of shoulder muscles may vary depending on the task. Future research methodologies should take a variety of environmental conditions into account in order to maximize the applicability of the results to typical everyday usage.

Nondisabled participants with no prior wheelchair experience were recruited for the current investigation. There are differences in propulsion technique between inexperienced and experienced wheelchair users and

their ways of adapting to the task environment at hand. These differences must be identified and accounted for so that we can extrapolate the results of the current investigation to experienced manual wheelchair users. Further studies to evaluate shoulder musculature function in different groups of daily wheelchair users, particularly those with various levels of SCI, would be informative. This work establishes a baseline in neurologically intact, inexperienced wheelchair users prior to assessment of the shoulder biomechanics and wheelchair kinetics in experienced neurologically impaired wheelchair users in order to limit variability secondary to medical conditions, including spinal cord or preexisting rotator cuff overuse attrition injuries. An identical test wheelchair was used for all nondisabled participants in this study. Studies have shown that wheelchair configuration influences wheelchair kinetics and shoulder muscle activation patterns [20–21]. Future work should consider using wheelchair users' own wheelchairs to determine the demands on shoulder musculature during wheelchair propulsion.

The study lacks kinematics data, preventing us from gaining any insight into the adjustments in trunk position that participants adopted to change their muscle coordination patterns. This is an important area to consider in future research investigating the effect of posture on muscle coordination. Trunk muscle activity patterns during incline propulsion should be considered in future studies [22].

CONCLUSIONS

The present study shows the differences in kinetics and EMG activity patterns of superficial shoulder muscles during level-ground and incline propulsion. EMG intensity of the push muscles increased significantly during incline propulsion, which corresponds with the increased kinetic data total force output in the incline propulsion condition. In addition, the significantly longer EMG duration of the push muscles (PM, AD, and BB) during incline propulsion coincided with the longer percent push phase. PCA was used to quantify the differences in the coordination patterns between level-ground and incline propulsion. The reconstructed EMG patterns using the first ten PCs showed EMG activities of push muscles (PM, AD, and BB) in the early push phase and late recovery phase during the level-ground propulsion, whereas in the incline propulsion, push muscles showed more intense and longer EMG activities in the push phase and less EMG activities of UT and MD. PCA is useful when the aim of the study is to quantitatively classify EMG patterns recorded across muscles. The application of PCA to EMG data shows that this method of capturing features from sEMG signals can provide insight not only into the activation state of motor units but also into the coordination of muscles, opening new windows for both neurophysiological and clinical/rehabilitation studies.

ACKNOWLEDGMENTS

Author Contributions:
Study concept and design: L. Qi, J. Wakeling, M. Ferguson-Pell.
Acquisition of data: L. Qi, M. Ferguson-Pell.
Analysis and interpretation of data: L. Qi, J. Wakeling.
Drafting of manuscript: L. Qi, J. Wakeling, S. Grange, M. Ferguson-Pell.
Critical revision of manuscript for important intellectual content: L. Qi, J. Wakeling, S. Grange, M. Ferguson-Pell.
Statistical analysis: L. Qi.
Obtained funding: L. Qi, M. Ferguson-Pell.
Administrative, technical, or material support: L. Qi, M. Ferguson-Pell.
Study supervision: L. Qi, S. Grange, M. Ferguson-Pell.
Financial Disclosures: The authors have declared that no competing interests exist.
Funding/Support: This material was based on work supported by a Dorothy Hodgkin Postgraduate Award, Engineering Physical Sciences Research Council, with support from the Royal National Orthopedic Hospital Special Trustees.
Institutional Review: All participants gave informed consent in accordance with the procedures approved by the University of Alberta Ethics Committee.
Participant Follow-up: The authors have no plans to notify the study subjects of the publication of this article because of a lack of contact information.

REFERENCES

1. Curtis KA, Drysdale GA, Lanza RD, Kolber M, Vitolo RS, West R. Shoulder pain in wheelchair users with tetraplegia and paraplegia. Arch Phys Med Rehabil. 1999;80(4):453–57. [PMID:10206610] http://dx.doi.org/10.1016/S0003-9993(99)90285-X
2. Kulig K, Rao SS, Mulroy SJ, Newsam CJ, Gronley JK, Bontrager EL, Perry J. Shoulder joint kinetics during the push phase of wheelchair propulsion. Clin Orthop Relat Res. 1998;(354):132–43. [PMID:9755772]
3. Veeger HE, Rozendaal LA, van der Helm FC. Load on the shoulder in low intensity wheelchair propulsion. Clin Biomech (Bristol, Avon). 2002;17(3):211–18.

[PMID:11937259]
http://dx.doi.org/10.1016/S0268-0033(02)00008-6

4. Lin HT, Su FC, Wu HW, An KN. Muscle forces analysis in the shoulder mechanism during wheelchair propulsion. Proc Inst Mech Eng H. 2004;218(4):213–21. [PMID:15376723] http://dx.doi.org/10.1243/0954411041561027
5. Sabick MB, Kotajarvi BR, An KN. A new method to quantify demand on the upper extremity during manual wheelchair propulsion. Arch Phys Med Rehabil. 2004;85(7): 1151–59. [PMID:15241767] http://dx.doi.org/10.1016/j.apmr.2003.10.024
6. Richter WM, Rodriguez R, Woods KR, Axelson PW. Stroke pattern and handrim biomechanics for level and uphill wheelchair propulsion at self-selected speeds. Arch Phys Med Rehabil. 2007;88(1):81–87. [PMID:17207680] http://dx.doi.org/10.1016/j.apmr.2006.09.017
7. Mulroy SJ, Farrokhi S, Newsam CJ, Perry J. Effects of spinal cord injury level on the activity of shoulder muscles during wheelchair propulsion: an electromyographic study. Arch Phys Med Rehabil. 2004;85(6):925–34. [PMID:15179646] http://dx.doi.org/10.1016/j.apmr.2003.08.090
8. Mulroy SJ, Gronley JK, Newsam CJ, Perry J. Electromyographic activity of shoulder muscles during wheelchair propulsion by paraplegic persons. Arch Phys Med Rehabil. 1996;77(2):187–93. [PMID:8607745] http://dx.doi.org/10.1016/S0003-9993(96)90166-5
9. von Tscharner V. Intensity analysis in time-frequency space of surface myoelectric signals by wavelets of specified resolution. J Electromyogr Kinesiol. 2000;10(6):433–45. [PMID:11102846] http://dx.doi.org/10.1016/S1050-6411(00)00030-4
10. Bosco G. Principal component analysis of electromyographic signals: An overview. Open Rehabil J. 2010;3: 127–31.
11. Boettcher CE, Ginn KA, Cathers I. Standard maximum isometric voluntary contraction tests for normalizing shoulder muscle EMG. J Orthop Res. 2008;26(12):1591–97. [PMID:18528827] http://dx.doi.org/10.1002/jor.20675
12. Kelly BT, Kadrmas WR, Kirkendall DT, Speer KP. Optimal normalization tests for shoulder muscle activation: an electromyographic study. J Orthop Res. 1996;14(4):647–53. [PMID:8764876] http://dx.doi.org/10.1002/jor.1100140421
13. Qi L, Wakeling J, Grange S, Ferguson-Pell M. Changes in surface electromyography signals and kinetics associated with progression of fatigue at two speeds during wheelchair propulsion. J Rehabil Res Dev. 2012;49(1):23–34. [PMID:22492335] http://dx.doi.org/10.1682/JRRD.2011.01.0009
14. Cowan RE, Boninger ML, Sawatzky BJ, Mazoyer BD, Cooper RA. Preliminary outcomes of the SmartWheel Users' Group database: a proposed framework for clinicians to objectively evaluate manual wheelchair propulsion. Arch Phys Med Rehabil. 2008;89(2):260–68. [PMID:18226649] http://dx.doi.org/10.1016/j.apmr.2007.08.141
15. Qi L, Wakeling JM, Green A, Lambrecht K, Ferguson-Pell M. Spectral properties of electromyographic and mechanomyographic signals during isometric ramp and step contractions in biceps brachii. J Electromyogr Kinesiol. 2011; 21(1):128–35. [PMID:21067944] http://dx.doi.org/10.1016/j.jelekin.2010.09.006
16. Boninger ML, Cooper RA, Robertson RN, Shimada SD. Three-dimensional pushrim forces during two speeds of wheelchair propulsion. Am J Phys Med Rehabil. 1997; 76(5):420–26. [PMID:9354497] http://dx.doi.org/10.1097/00002060-199709000-00013
17. Bernasconi SM, Tordi N, Ruiz J, Parratte B. Changes in oxygen uptake, shoulder muscles activity, and propulsion cycle timing during strenuous wheelchair exercise. Spinal Cord. 2007;45(7):468–74. [PMID:17060923] http://dx.doi.org/10.1038/sj.sc.3101989
18. Chow JW, Millikan TA, Carlton LG, Chae WS, Lim YT, Morse MI. Kinematic and electromyographic analysis of wheelchair propulsion on ramps of different slopes for young men with paraplegia. Arch Phys Med Rehabil. 2009; 90(2):271–78. [PMID:19236980] http://dx.doi.org/10.1016/j.apmr.2008.07.019
19. U.S. Department of Justice. Americans with Disabilities Act standards for accessible design. Washington (DC): U.S. Department of Justice; 1994.
20. Louis N, Gorce P. Surface electromyography activity of upper limb muscle during wheelchair propulsion: Influence of wheelchair configuration. Clin Biomech (Bristol, Avon). 2010;25(9):879–85. [PMID:20846767] http://dx.doi.org/10.1016/j.clinbiomech.2010.07.002
21. Boninger ML, Baldwin M, Cooper RA, Koontz A, Chan L. Manual wheelchair pushrim biomechanics and axle position. Arch Phys Med Rehabil. 2000;81(5):608–13. [PMID:10807100] http://dx.doi.org/10.1016/S0003-9993(00)90043-1
22. Howarth SJ, Polgar JM, Dickerson CR, Callaghan JP. Trunk muscle activity during wheelchair ramp ascent and the influence of a geared wheel on the demands of postural control. Arch Phys Med Rehabil. 2010;91(3):436–42. [PMID:20298836] http://dx.doi.org/10.1016/j.apmr.2009.10.016

Submitted for publication June 8, 2012. Accepted in revised form October 29, 2012.

This article and any supplementary material should be cited as follows:
Qi L, Wakeling J, Grange S, Ferguson-Pell M. Coordination patterns of shoulder muscles during level-ground and incline wheelchair propulsion. J Rehabil Res Dev. 2013; 50(5):651–62.
http://dx.doi.org/10.1682/JRRD.2012.06.0109

ResearcherID/ORCID: Liping Qi, PhD: D-2061-2013; Martin Ferguson-Pell, PhD: A-2326-2012